Lecture Note #5: Direct Detection of DM

David Morrissey
October 21, 2015

Having spent a considerable amount of time discussing the creation of dark matter, we turn next to investigate ways to detect it. Our galaxy is surrounded by a halo of dark matter (DM). Every so often, a DM particle in the halo might scatter off an atomic nucleus and produce an observable signal. Looking for DM in this way is called direct detection (DD). In this note we describe how to compute this signal, and we outline the current experimental status of direct dark matter searches.

1 Dark Matter and Us

The DM in the Milky-Way halo has a distribution of densities and velocities. At our location in the galaxy the local energy density of DM is estimated to be $\rho_\odot \simeq 0.3$ GeV/cm^3. Simulations of the DM halo suggest that the velocity distribution reaches a steady state that is approximately Gaussian:

$$f(\vec{v}) \simeq \left(\frac{1}{\pi v_0^2}\right)^{3/2} e^{-v^2/v_0^2} \times N\,\Theta(v_{esc}-v)\ , \tag{1}$$

with $v_0 \simeq 220\,\mathrm{km/s}$. The second factor includes a step function to account for the fact that DM particles with speed $v > v_{esc}$ can escape the galaxy, as well as factor of $N \simeq 1$ to correct the normalization of the truncated distribution to unity ($\int d^3v\ f(\vec{v}) = 1$).

Most of the visible material in our galaxy is located in the galactic disk. It is about 0.3 pc thick, roughly 20 kpc in radius, and is rotating about the galactic center relative to the apparently stationary galactic halo. Our star, the Sun, is located in the disk about 8.5 kpc from the galactic center, and is rotating along with everything else. We illustrate the situtation in Fig. 1. Due to the motion of the sun together with our own motion relative to the sun, we have a net speed relative to the DM halo of

$$v_E \simeq 230\,\mathrm{km/s} + (15\,\mathrm{km/s})\cos[\omega(t-t_0)]\ , \tag{2}$$

where the first term comes from the motion of the sun with the galatic rotation and the second from the orbital motion of the Earth around the Sun. Not surprisingly the frequency is $\omega = 1/(1\,\mathrm{yr})$, while the phase is such that the relative motion is maximized on $t_0 = \mathrm{June}\,2$.

The distribution of DM velocities in the halo together with our net motion relative to the halo imply that we see a net flux of DM. This flux can scatter off targets in the laboratory, potentially producing an observable signal.

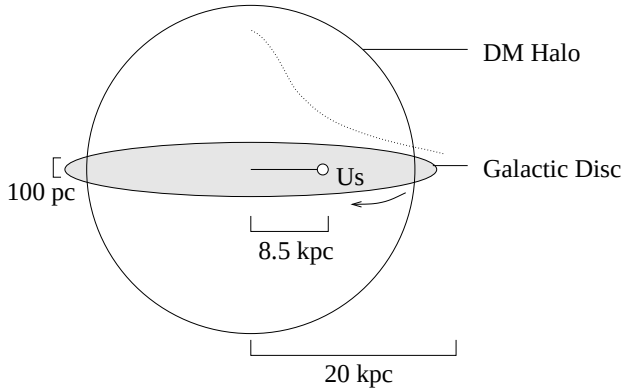

Figure 1: Cartoon of our galaxy, including the DM halo. (Note: not to scale!)

2 Scattering Rates off Nuclei

The quantity of interest for DM direct detection is the rate of nuclear recoils per unit recoil energy per unit detector mass. This rate is just the convolution of the DM flux with the differential scattering cross section, multiplied by the target density. Specifically, we have

$$\frac{dR}{dE_R} = n_T \left(\frac{\rho_\chi}{m_\chi}\right) \int d^3v'\, v'\, f_{lab}(\vec{v}')\, \frac{d\sigma_N}{dE_R} \ , \tag{3}$$

where n_T is the density per unit mass of the target nucleus, $d\sigma_N/dE_R$ is the differential DM-nucleus scattering cross section, and $f_{lab}(\vec{v}')$ is the distribution of DM velocities $\vec{v}'$ in the lab frame. Note that this distribution is slightly different from the halo-frame distribution given in Eq. (1). However, since $\vec{v}' = \vec{v} + \vec{v}_E$, we have $d^3v = d^3v'$ and

$$f_{lab}(\vec{v}') = f(\vec{v}' - v_E) \ . \tag{4}$$

The only thing left to specify is the differential cross section.

Before attempting to compute the cross section, it is worth examining the kinematics of a DM-nucleus scattering event. A typical event consists of a DM particle from the halo with speed $v \sim 10^{-3}$ colliding with a nucleus that is effectively at rest. In the lab frame, the momentum transferred to the nucleus is

$$q = 2\mu_N\, v\, \cos\theta \ , \tag{5}$$

where $\mu_N = m_N m_\chi/(m_N + m_\chi)$ is the DM-nucleus reduced mass and $\theta \in [0, \pi/2]$ is the angle of the scattered nucleus relative to the initial DM direction, as illustrated in Fig. 2. For $m_\chi \sim m_N \sim 100$ GeV, the typical momentum transfer is $q \sim 100$ MeV. The kinetic energy imparted to the recoiling nucleus is

$$E_R = \frac{q^2}{2m_N} = \frac{2\mu_N^2 v^2 \cos^2\theta}{m_N} \ , \tag{6}$$

which implies $E_R \sim 100$ keV for typical masses. Fortunately, nuclear recoil energies of this size can be probed by a number of existing detector technologies.

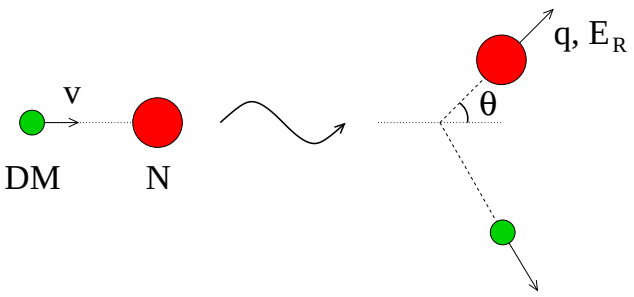

Figure 2: Kinematics of direct detection.

3 DM-Nucleus Scattering Cross Sections

Computing a DM-nucleus scattering cross section involves three steps. Starting from a theory of DM, the first step is to determine how the DM particle χ couples to quarks and gluons. The second step is to convert this interaction among elementary particles to a coupling of χ to composite nucleons. Once this is done, the DM-nucleon coupling must then be translated into an effective interaction between χ and the even-more composite target nucleus of interest. These three steps require aspects of elementary particle physics, hadronic physics, and nuclear physics.

Just like there are many possible DM candidates, there are also many ways by which a DM particle can interact with quarks and gluons. Some popular examples for a fermionic DM particle χ are:

$$\text{SS}: \quad d_q\, \bar{\chi}\chi\, \bar{q}q, \quad d_G\, \bar{\chi}\chi\, G^a_{\mu\nu} G^{a\,\mu\nu}, \tag{7}$$

$$\text{VV}: \quad b_q\, \bar{\chi}\gamma^\mu\chi\, \bar{q}\gamma_\mu q, \tag{8}$$

$$\text{AA}: \quad a_q\, \bar{\chi}\gamma^\mu\gamma^5\chi\, \bar{q}\gamma_\mu\gamma^5 q\ . \tag{9}$$

These are all higher-dimensional operators, and thus the couplings d_q, b_q, a_q must have mass dimension equal to minus two, while the d_g coupling to gluons has mass dimension of minus three.[1] The labels SS, VV, and AA refer to the spin and parity of the fermion bilinears they contain: SS stands for scalar-scalar ($\bar{f}f$ is a Lorentz scalar), VV stands for vector-vector ($\bar{f}\gamma^\mu f$ is a Lorentz vector), and AA stands for axialvector-axialvector ($\bar{f}\gamma^\mu\gamma^5 f$ is a Lorentz axialvector). A similar classification can be used when the DM particle is a boson.

These operators should be thought of as low-energy effective interactions rather than fundamental couplings. The SS operators can be induced by the exchange of a heavy scalar boson (such as a Higgs), while the VV operators can be generated by the exchange of a heavy vector (such as the Z^0). This is an excellent approximation when the momentum exchanged $q \sim (100\text{ MeV})$ is much smaller than the mass M of the mediator particle. In this case, d_q, b_q, $a_q \propto g_\chi g_q / M^2$, where $g_{\chi,q}$ are the couplings of the mediator to DM and quarks. The

[1] Recall that any operator in the Lagrangian must have a mass dimension of four, and that fermion fields have mass dimension 3/2 and boson fields have mass dimension one.

coupling to gluons in Eq. (7) can be generated by a DM coupling to heavy quarks (like the top) that is closed into a loop and connected to a pair of gluons.

Besides SS, VV, and AA operators, we could also have mixtures like VA or other Lorentz structures such as PP (P = pseudoscalar – $\bar{f}\gamma^5 f$). These are not usually considered because they predict scattering cross sections that are proportional to the momentum transfer or the DM velocity. Since these quantities are numerically very small ($v^2 \sim 10^{-6}$), DM scattering through Lorentz structures other than SS, VV, and AA are expected to be very suppressed. These conclusions also carry through for bosonic DM particles.

3.1 Spin-Independent Scattering – SS

The SS and VV operators give rise to *spin-independent* (SI) scattering of DM, where the total DM-nucleus coupling is a coherent superposition of the DM couplings to individual nucleons. These couplings are therefore able to produce much larger scattering rates than interactions that do not have this coherent property, and many of the experimental searches for DM have concentrated on them.

Consider first the SS operators $d_q \bar{q}q\, \bar{\chi}\chi$, $d_Q \bar{Q}Q\, \bar{\chi}\chi$, and $d_G\, G^a_{\mu\nu} G^{a\,\mu\nu}\, \bar{\chi}\chi$, where $q = u,\, d,\, s$ refer to the light quarks and $Q = c,\, b,\, t$ refer to the heavy quarks. If we were interested only in the scattering of DM with quarks or gluons, it would be straightforward to compute the corresponding cross sections. Instead, we need to find the scattering with nucleons induced by these operators. Once we have this, we can convert them into scattering cross sections with nuclei.

As a warm up, let us first do the case of χ scattering with a quark mediated by the operator $d_q\, \bar{q}q\; \bar{\chi}\chi$. Since this is just an example, we will pretend that the quark is a free particle with mass m_q. The matrix element for the process $\chi(p_1) + q(p_2) \to \chi(p_3) + q(p_4)$ from this operator is[2]

$$\begin{aligned} \mathcal{M} &= \langle q(p_4)\chi(p_3)|\, d_q\, \bar{q}q\; \bar{\chi}\chi\, |\chi(p_1)q(p_2)\rangle & (10)\\ &\simeq d_q\, \langle q(p_4)|\, \bar{q}q\, |q(p_2)\rangle\, \langle \chi(p_3)|\, \bar{\chi}\chi\, |\chi(p_1)\rangle & (11)\\ &= \kappa\, d_q\, \bar{u}(p_4, s_4) u(p_2, s_2)\, \bar{u}(p_3, s_3) u(p_1, s_1)\ , & (12) \end{aligned}$$

where the $u(p, s)$ factors are four-component spin polarizations and $\kappa = 1$ (2) if χ is Dirac (Majorana). [3] In the extreme non-relativistic limit, where all momenta are much smaller than the masses, the summed and squared matrix element (averaged over initial states and summed over final states) in this case reduces to

$$\text{“}|\mathcal{M}|^{2\prime\prime} = \kappa^2\, d_q^2\, (4 m_q m_\chi)^2\ . \tag{13}$$

All this should be familar from your QFT class.

[2] Here and in the the discussion to follow, the matrix elements of position-space operators are implicitly Fourier-transformed into momentum space to give the scattering matrix elements.

[3] In the Majorana case, there are two contractions of the operator instead of the one for Dirac, and the κ factor accounts for this.

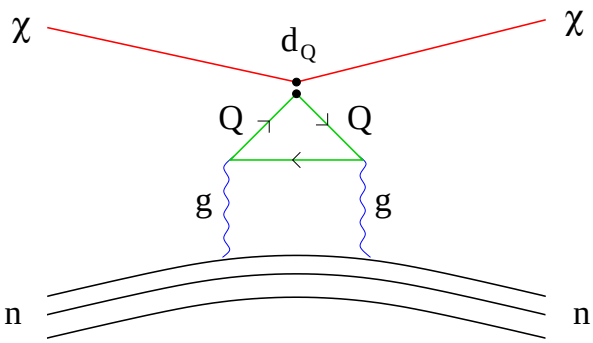

Figure 3: Diagram representing the loop connecting the $d_Q\,\bar{Q}Q\bar{\chi}\chi$ operator to a gluon effective operator with nucleons.

The next step is to convert this result into scattering with a nucleon n, where $n = p,\, n$.[4] For the light quarks, $q = u,\, d,\, s$, it can be shown that at low momentum transfer ($q \ll m_n$)

$$\langle n(p_4)|\,\bar{q}q\,|n(p_2)\rangle = \frac{m_n}{m_q} f_{T_q}^{(n)}\;\bar{u}_4 u_2\;, \tag{14}$$

where $f_{T_q}^{(n)}$ is a coefficient that must be extracted non-perturbatively and $\bar{u}_4 u_2 = \bar{u}(p_4, s_4)u(p_2, s_2)$ is a convenient shorthand for the spin polarizations of the initial and final nucleons. This result is just like what we had for the case of quark scattering, but with an additional prefactor ($f_{T_q}^{(n)}$) and the initial and final quark states replaced by nucleon states.

Nucleon scattering can also be induced by operators with heavy quarks or gluons. In the case of the gluonic operator $d_G\,\bar{\chi}\chi\,G^a_{\mu\nu}G^{a\,\mu\nu}$, the corresponding result at low-momentum transfer ($q \ll m_n$) is

$$\langle n(p_4)|\,G^a_{\mu\nu}G^{a\,\mu\nu}\,|n(p_2)\rangle = -\frac{8\pi}{9\alpha_s} f_{T_G}^{(n)} m_n\;\bar{u}_4 u_2\;, \tag{15}$$

where $\alpha_s = g_s^2/4\pi$ is the strong coupling, and the nucleon spin polarization stuff is the same as before. The coefficient $f_{T_G}^{(n)}$ in this expression can be shown to be related to the coefficients of the light quarks according to

$$f_{T_G}^{(n)} = 1 - \sum_{q=u,d,s} f_{T_q}^{(n)}\;. \tag{16}$$

The derivation of this relation will be covered in a tutorial.

The heavy quark operators $d_Q\bar{Q}Q\,\bar{\chi}\chi$, $Q = c,\, b,\, t$, also contribute to nucleon scattering. They do so through loops that connect the heavy quarks to a pair of gluons, as shown in Fig. 3. As far as nucleon matrix elements are concerned, the net result of these loops is to make the replacements

$$\bar{Q}Q \to -\frac{2\alpha_s}{24\pi\, m_Q}\, G^a_{\mu\nu}G^{a\,\mu\nu}\;. \tag{17}$$

[4] Sorry about the abuse of notation.

We are now ready to put everything together.

Suppose the complete set of SS effective couplings is

$$-\mathscr{L} \supset \sum_{q=u,d,s} d_q\, \bar{q}q\, \bar{\chi}\chi \quad + \quad \sum_{Q=c,b,t} d_Q\, \bar{Q}Q\, \bar{\chi}\chi \quad + \quad d_G\, G^a_{\mu\nu} G^{a\,\mu\nu}\, \bar{\chi}\chi \ . \tag{18}$$

For low momentum transfer ($q \ll m_n$), this gives the summed and squared matrix element

$$\text{“}|\mathcal{M}|^{2\prime\prime} = \kappa^2 f_n^2\, (4 m_n m_\chi)^2 \ , \tag{19}$$

where the effective χ-nucleon coupling f_n ($n = p,\, n$) is

$$\frac{f_n}{m_n} = \sum_{q=u,d,s} f^{(n)}_{T_q} \frac{d_q}{m_q} \ + \ \frac{2}{27} \sum_{Q=c,b,t} f^{(n)}_{T_G} \frac{d_Q}{m_Q} \ - \ \frac{8\pi}{9\alpha_s} d_G f^{(n)}_{T_G} \ . \tag{20}$$

This result is equivalent to writing an effective Lagrangian that couples the DM particle χ directly to nucleons:

$$-\mathscr{L}_{eff} \supset f_p\, \bar{\chi}\chi\, \bar{p}p + f_n\, \bar{\chi}\chi\, \bar{n}n \ , \tag{21}$$

with f_p and f_n given by Eq. (20). Note that this effective Lagrangian is only valid for low momentum transfers, $q \ll m_n$. It is now straightforward to integrate the summed and squared matrix element over phase space to get the differential cross section

$$\frac{d\sigma_n}{dq^2} = \frac{\kappa^2}{4\pi} \frac{1}{v^2} f_n^2 \ , \tag{22}$$

where $q = |\vec{p}_4|$ is the momentum of the outgoing nucleon.

The third and final step is to convert the nucleon result to a scattering cross section with a nucleus, comprised of Z protons and $(A-Z)$ neutrons. For SI operators, the contributions to the amplitude from each of the constituent nucleons add coherently at zero momentum transfer. This implies

$$\left.\frac{d\sigma}{dq^2}\right|_{q^2=0} = \quad \frac{\kappa^2}{4\pi} \frac{1}{v^2} \left[Z f_p + (A-Z) f_n\right]^2 \ . \tag{23}$$

When the momentum transfer approaches the inverse size of a nucleon, the DM collision starts to become sensitive to the underlying nucleon structure of the nucleus and some of the coherence is lost. To account for this, a form factor $F(E_R)$ is introduced,

$$\frac{d\sigma}{dE_R} = 2 m_N \left.\frac{d\sigma}{dq^2}\right|_{q^2=0} F_N^2(E_R) \ , \tag{24}$$

where the factor of $2m_N$ converts between E_R and q^2. The form factor $F_N(E_R)$ can be related to the Fourier transform of the nucleon density. A popular approximation is the *Woods-Saxon* form:

$$F_N^2(E_R) = \left[\frac{3 j_1(qR_1)}{qR_1}\right]^2 e^{-(qs)^2} \ , \tag{25}$$

where $s \simeq 1\,\text{fm}$, j_1 is a spherical Bessel function, $q = \sqrt{2m_N E_R}$, and $R_1 = \sqrt{R^2 - 5s^2}$ for $R = 1.2\,A^{1/3}\,\text{fm}$.

Even though $d\sigma_N/dE_R$ depends on the recoil energy through the form nuclear form factor, it is standard practice to define an effective energy-independent nuclear scattering cross section $\bar{\sigma}_N$ by

$$\bar{\sigma}_N = \int_0^{4\mu_N^2 v^2} dq^2 \; \left.\frac{d\sigma}{dq^2}\right|_{q^2=0} = \frac{\kappa^2}{\pi}\,\mu_N^2\,\left[Z f_p + (A-Z) f_n\right]^2 \; . \tag{26}$$

3.2 Spin-Independent Scattering – VV

Computing the nuclear scattering cross section from a VV operator of the form $b_q\,\bar{\chi}\gamma^\mu\chi\;\bar{q}\gamma_\mu q$ is very similar to the SS case discussed above, but with a few nice simplifications. These are related to the fact that for any fermion f, the operator $j_f^\mu = \bar{f}\gamma^\mu f$ is the number density current, with j_f^0 being the number density of fermions minus antifermions, and $\vec{j}_f$ the spatial number current. On the SM side, this implies that the $\bar{q}\gamma_\mu q$ part of the operator is closely related to the electromagnetic current density, which we know is conserved. On the DM side, the important implication is that $\bar{\chi}\gamma^\mu\chi$ vanishes when χ is a Majorana fermion with no distinct antiparticle.

Following our previous treatment, consider first the elastic scattering of χ with a quark q at low momentum transfer ($q \ll m_q,\, m_\chi$). The matrix element is

$$\mathcal{M} = b_q\,\bar{u}(p_4,s_4)\gamma^\mu u(p_2,s_2)\,\bar{u}(p_3,s_3)\gamma_\mu u(p_1,s_1) \; . \tag{27}$$

Doing the spin sums and averages, this becomes

$$\text{“}|\mathcal{M}|^{2\prime\prime} = b_q^2 (4 m_q m_\chi)^2 \; . \tag{28}$$

Nothing new here.

To convert this result to scattering with a nucleon and then with a nucleus, we can make use of the nice property of the SM part of the VV operator. Since this operator just counts the net quark content, the effective DM-nucleon operator is just

$$-\mathscr{L}_{eff} \supset f_p\,\bar{\chi}\chi\,\bar{p}p + f_n\,\bar{\chi}\chi\,\bar{n}n \; , \tag{29}$$

with

$$f_p = 2b_u + b_d \quad (n = p = uud) \tag{30}$$

$$f_n = b_u + 2b_d \quad (n = n = udd) \; . \tag{31}$$

The same trick works for converting the nucleon effective interaction to a scattering cross section with nuclei, although we still need to include a form factor to account for a loss of coherence at high energies. This form factor can be related to the Fourier transform of the charge density in the nucleus. Since the charge density of a nucleus is usually expected to trace the mass density, many analyses use the same Woods-Saxon form factor of Eq. (25). With this additional approximation, the final result is then identical to the SS case, and Eqs. (23,24) carry through to the VV case here as well.

3.3 Spin-Dependent Scattering – AA

The AA operator leads to an interaction between χ and the spin of a nucleon. Thus, when this nucleon effective interaction is converted into a total interaction with the target nucleus, the contributions from the nucleon constituents no longer combine in a coherent way. Instead, the induced nuclear interaction depends on the net spin state of the nucleus. Thus, scattering mediated by AA operators is said to be *spin-dependent* (SD).

Going between the quark-level operator and the nucleon operator for the AA interaction is a bit more complicated than for the SS and VV cases. As before, we consider the matrix element of the $\bar{q}q$ operator between a pair of nucleons $n = p,\, n$:

$$\langle n(p_4)|\, \bar{q}\gamma^\mu\gamma^5 q\, |n(p_2)\rangle = 2\Delta q^{(n)}\, \bar{u}_4 s^\mu u_2 \ , \tag{32}$$

where s^μ is the nucleon spin operator and $\Delta q^{(n)}$ corresponds to the contribution of the quark flavour q to the net nucleon spin. In the extreme non-relativistic limit, the spin operator reduces to the familiar one-particle quantum-mechanical form, $s^\mu \to (0, \vec{J})$. Only the light quarks ($q = u, d, s$) are expected to give non-negligible values of $\Delta q^{(n)}$, whose numerical values are extracted experimentally.

The result of Eq. (32) can be rewritten in terms of an effective nucleon interaction. Starting from the AA quarks operators, the corresponding effective Lagrangian is

$$-\mathscr{L}_{eff} \supset 2\sqrt{2}G_F\, a_p\, \bar{\chi}\gamma^\mu\gamma^5\chi\, \bar{p}s_\mu p + 2\sqrt{2}G_F\, a_n\, \bar{\chi}\gamma^\mu\gamma^5\chi\, \bar{n}s_\mu n \ , \tag{33}$$

where

$$a_n = \sum_{q=u,d,s} \frac{a_q}{\sqrt{2}G_F}\Delta q^{(n)} \qquad (n = p,\, n) \ . \tag{34}$$

The factors of the Fermi constant G_F are conventional, and they make the a_n coefficients dimensionless.

The next step is to convert the nucleon result to a matrix element for the target nucleus. As for the SI operators, we will first compute the result at zero momentum transfer, and then add a form factor to account for non-zero q^2. With $q^2 \to 0$, the nuclear matrix elements of the nucleon operators are ($n = p,\, n$)

$$\langle S_n^\mu\rangle = \langle N|\, \bar{n}s^\mu n\, |N\rangle \ , \tag{35}$$

where S_n^μ is the contribution to the spin of the nucleus from the proton or the neutron. The sum of these contributions can be related to the total nuclear spin by the Wigner-Eckart theorem [1, 4], to give

$$a_p\langle S_p^\mu\rangle + a_n\langle S_n^\mu\rangle = \Lambda\, \langle N|\, S^\mu\, |N\rangle \ , \tag{36}$$

where S^μ is the total spin operator of the nucleus, with $S^\mu \to (0, \vec{J})$ in the non-relativistic limit, and Λ is a constant of proportionality. To determine Λ, suppose we evaluate both sides of Eq. (36) with $\mu = 3 = z$ between nuclear states with $m_J = J$:

$$\Lambda = \frac{1}{J}\left(a_p\langle S_p\rangle + a_n\langle S_n\rangle\right) \ , \tag{37}$$

where $\langle S_p \rangle := \langle N; J, m_J = J | \, S_p^z \, | N; J, m_J = J \rangle$ and similarly for n. Values of $\langle S_p \rangle$ and $\langle S_n \rangle$ are tabulated for various types of nuclei.

We now have everything we need to compute the differential cross section at zero momentum transfer.[5] The result is

$$\left.\frac{d\sigma_N}{dq^2}\right|_{q^2=0} = \frac{2\kappa^2}{\pi}\frac{G_F^2}{v^2}\Lambda^2 J(J+1) \ , \tag{38}$$

where J is the total spin state of the target nucleus, and $\kappa = 1$ (2) for a Dirac (Majorana) χ. To get the result at non-zero momentum transfer, we just multiply by a form factor

$$\frac{d\sigma_N}{dE_R} = 2m_N \left.\frac{d\sigma_N}{dq^2}\right|_{q^2=0} \frac{S(q^2)}{S(0)} \ , \tag{39}$$

with

$$S(q^2) = a_0^2 S_{00}(q^2) + a_0 a_1 S_{01}(q^2) + a_{11} S_{11}(q^2) \ , \tag{40}$$

where $a_0 = a_p + a_n$ and $a_1 = a_p - a_n$ are the nuclear-isospin singlet and triplet combinations. The functions $S_{ij}(q^2)$ have been computed for various nuclei and can be looked up.

As in the SI case, it is conventional to define an effective SD nuclear cross section by

$$\bar{\sigma}_N^{SD} = 4\mu_N v^2 \left.\frac{d\sigma_N}{dq^2}\right|_{q^2=0} = \frac{8\kappa^2}{\pi} G_F^2 \, \mu_N^2 \Lambda^2 J(J+1) \ . \tag{41}$$

4 Experimental Status

Many experiments have attempted to discover dark matter through direct detection. Some have even found an excess of events over the expected background, but the situation is far from clear. We will attempt to give an overview of the latest results.

4.1 Limits on SI Scattering

The strongest limits on DM direct detection come from searches for SI scattering. These scattering rates can be enhanced by a factor of A^2 (or more) at low energies for the case of $f_p = f_n$. Thus, many experiments use very heavy target nuclei to maximize this enhancement. Since different experiments use different target materials, it is convenient to define an effective SI cross section per nucleon so that we may compare the limits from different experiments. The relevant quantity is

$$\sigma_{SI} = \frac{1}{A^2}\frac{\mu_p^2}{\mu_N^2}\,\bar{\sigma}_N = \frac{\kappa^2}{\pi}\mu_p^2 \, \frac{\left[Z f_p + (A-Z) f_n\right]^2}{A^2} \ , \tag{42}$$

[5] You'll do this yourself in a tutorial.

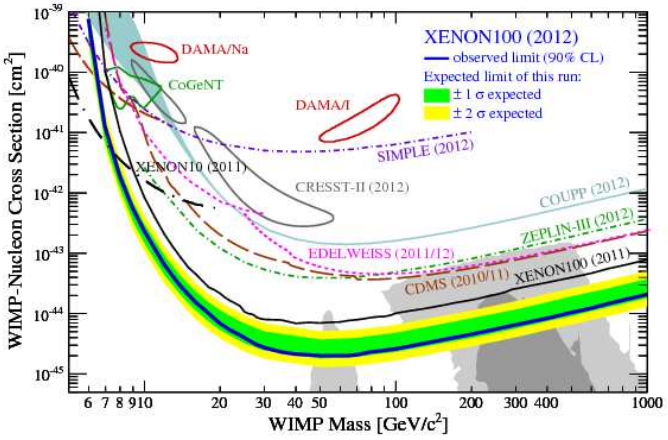

Figure 4: SI DD from xenon

where μ_p is the DM-proton reduced mass.

For DM masses above about 10 GeV, the best current limits on SI scattering come from the XENON100 experiment. We show the excluded region in Fig. 4. As the name of the experiment suggests, the target material in the detector is xenon, with an atomic mass in the range of $A = 131$ (there are several stable isotopes), which gives a strong enhancement of the nuclear cross section. The shape of the excluded region is easy to understand. At lower DM masses, below about 50 GeV, $\mu_N \to m_\chi$ and the recoil energy of the target xenon nucleus begins to fall below the lower energy detection threshold of the experiment. Going to higher masses, the local number density ρ_χ/m_χ becomes smaller leading to fewer expected scattering events.

While XENON100 gives very strong limits on SI scattering, a few other experiments have found event rates that are larger than the expected backgrounds. The most visible of these is the DAMA/Libra experiment, whose target is mainly NaI crystals [6]. This experiment searches specifically for the annual modulation in scattering rates that is expected for DM due to the variation in the DM flux with the motion of the Earth around the Sun. As can be seen in Fig. 5, they do indeed find a significant modulation in their data. Moreover, the phase of this modulation is consistent with the expectation for DM, with a maximum near June 2 and a minimum near December 2. Many proposals have been made for a non-DM explanation for their result, some of which have been ruled out [7], and others that are still viable [8]. Other excesses are seen in the CoGeNT [9] and CRESST II [10] experiments.

An interpretation of these results in terms of DM with spin-independent scattering with nuclei does not appear to work. In Fig. 6, we show a plot of the regions consistent with a SI interpretation of the DAMA, CoGeNT, and CRESST II excesses together with the regions excluded by other experiments. Although these exclusions are subject to a number of systematic uncertainties, a SI explanation for the excesses seems to be ruled out. On the other hand, non-standard SI scattering may be able to account for at least some of the excesses while remaining consistent with other exclusions [11].

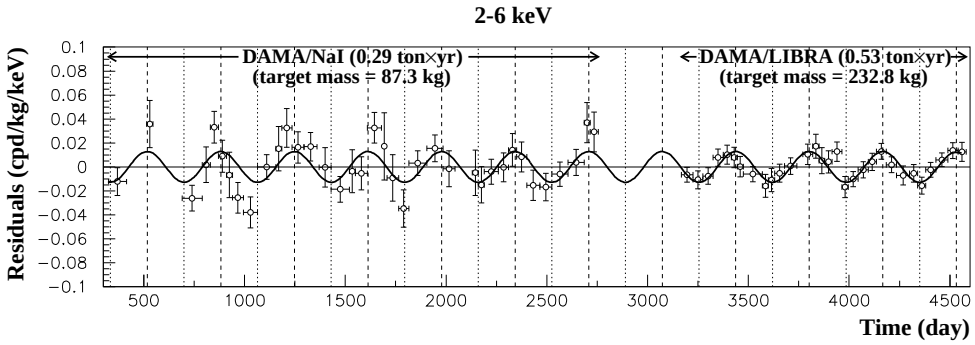

Figure 5: Time variation of the scattering rate seen in the DAMA/NaI and DAMA/LIBRA experiments. Plot from Ref. [6].

4.2 Limits on SD Scattering

Many experiments have also searched for SD scattering of DM using a variety of target materials. To allow for a direct comparison of these results, it is also standard practice to define effective SD cross sections for a single proton or neutron:

$$\bar{\sigma}^{SD}_{p,n} \;=\; \frac{6\kappa^2}{\pi} G_F^2\, \mu^2_{p,n}\, a^2_{p,n} \;, \tag{43}$$

where we have used $J = 1/2$ and $\langle S_p \rangle = \langle S_n \rangle = 1/2$. Limits derived from nuclear data can then be translated into limits on $\bar{\sigma}^{SD}_{p,n}$ [13]. Frequently, this is done in an approximate way by assuming that only one of a_p or a_n is non-zero and deriving the corresponding limit on $\sigma^{SD}_{p,n}$ under this assumption. We show these in Fig. 7, taken from Ref. [14].

References

[1] G. Jungman, M. Kamionkowski, K. Griest and , "Supersymmetric dark matter," Phys. Rept. **267**, 195 (1996) [hep-ph/9506380].

[2] J. Engel, S. Pittel, P. Vogel and , "Nuclear physics of dark matter detection," Int. J. Mod. Phys. E **1**, 1 (1992).

[3] P. Salati, "Indirect and direct dark matter detection," PoS CARGESE **2007**, 009 (2007).

[4] P. Agrawal, Z. Chacko, C. Kilic, R. K. Mishra and , arXiv:1003.1912 [hep-ph].

[5] E. Aprile *et al.* [XENON100 Collaboration], Phys. Rev. Lett. **109**, 181301 (2012) [arXiv:1207.5988 [astro-ph.CO]].

[6] R. Bernabei *et al.* [DAMA Collaboration], "First results from DAMA/LIBRA and the combined results with DAMA/NaI," Eur. Phys. J. C **56**, 333 (2008) [arXiv:0804.2741 [astro-ph]]; R. Bernabei *et al.* [DAMA and LIBRA Collaborations], "New results from DAMA/LIBRA," Eur. Phys. J. C **67**, 39 (2010) [arXiv:1002.1028 [astro-ph.GA]].

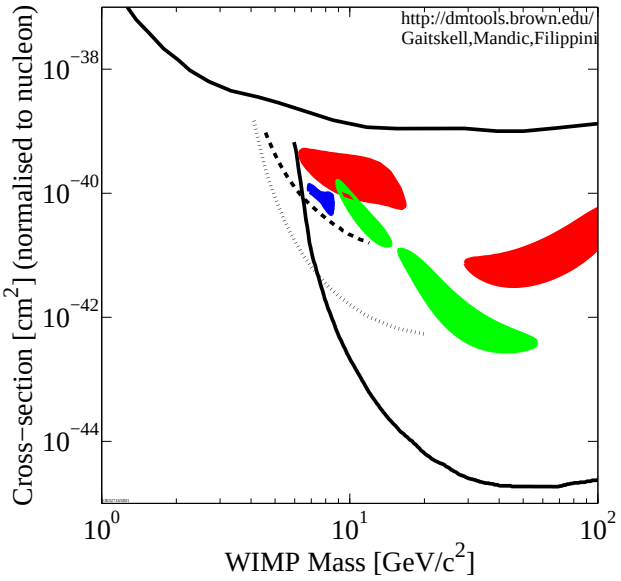

Figure 6: Limits on SI DM scattering from XENON100 (lower solid), XENON10 (dotted), CDMS (dashed), and CRESST I (upper solid). Also shown are the best-fit regions for DAMA (red filled), CoGeNT (blue filled), and CRESST II (green filled). This plot was made with tools of Ref. [12].

[7] S. Chang, J. Pradler, I. Yavin and , "Statistical Tests of Noise and Harmony in Dark Matter Modulation Signals," Phys. Rev. D **85**, 063505 (2012) [arXiv:1111.4222 [hep-ph]].

[8] J. Pradler, B. Singh, I. Yavin and , "On an unverified nuclear decay and its role in the DAMA experiment," Phys. Lett. B **720**, 399 (2013) [arXiv:1210.5501 [hep-ph]].

[9] C. E. Aalseth *et al.* [CoGeNT Collaboration], "Results from a Search for Light-Mass Dark Matter with a P-type Point Contact Germanium Detector," Phys. Rev. Lett. **106**, 131301 (2011) [arXiv:1002.4703 [astro-ph.CO]]; C. E. Aalseth, P. S. Barbeau, J. Colaresi, J. I. Collar, J. Diaz Leon, J. E. Fast, N. Fields and T. W. Hossbach *et al.*, "Search for an Annual Modulation in a P-type Point Contact Germanium Dark Matter Detector," Phys. Rev. Lett. **107**, 141301 (2011) [arXiv:1106.0650 [astro-ph.CO]].

[10] G. Angloher, M. Bauer, I. Bavykina, A. Bento, C. Bucci, C. Ciemniak, G. Deuter and F. von Feilitzsch *et al.*, "Results from 730 kg days of the CRESST-II Dark Matter Search," Eur. Phys. J. C **72**, 1971 (2012) [arXiv:1109.0702 [astro-ph.CO]].

[11] For example,
S. Chang, N. Weiner, I. Yavin and , "Magnetic Inelastic Dark Matter," Phys. Rev. D **82**, 125011 (2010) [arXiv:1007.4200 [hep-ph]].

[12] A fun website that makes plots of experimental limits on direct detection:
http://dmtools.brown.edu/ .

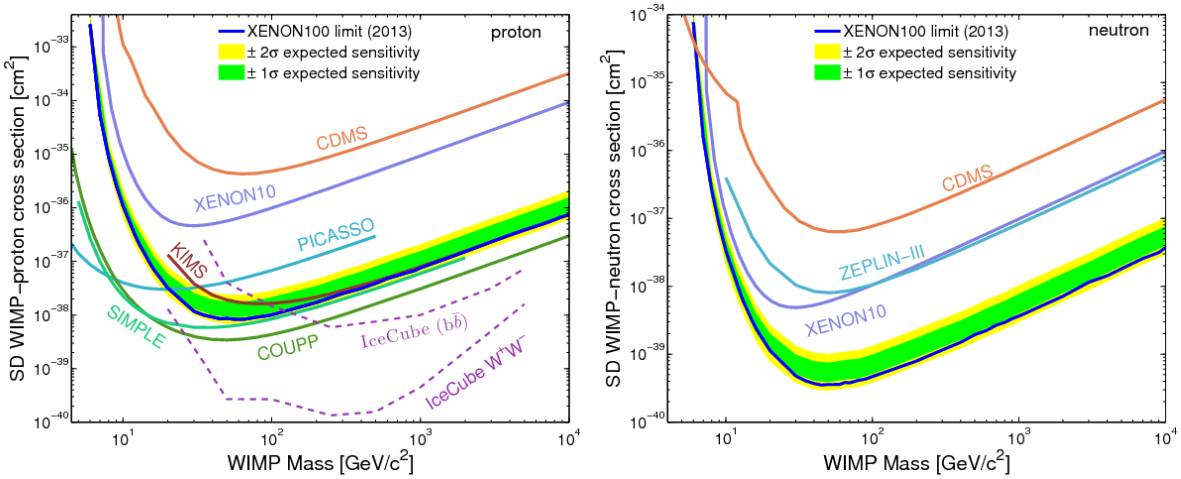

Figure 7: Limits on SD scattering of DM on nuclei. Plots from Ref. [14].

[13] D. R. Tovey, R. J. Gaitskell, P. Gondolo, Y. A. Ramachers, L. Roszkowski and , "A New model independent method for extracting spin dependent (cross-section) limits from dark matter searches," Phys. Lett. B **488**, 17 (2000) [hep-ph/0005041].

[14] [XENON100 Collaboration], "Limits on spin-dependent WIMP-nucleon cross sections from 225 live days of XENON100 data," arXiv:1301.6620 [astro-ph.CO].